ISSN 1674-1056
http://cpb.iphy.ac.cn
http://iopscience.iop.org/cpb
中国物理 B
Chinese Physics
中国物理
Chinese Physics B

Quantitative and sensitive detection of prohibited fish drugs by surface-enhanced Raman scattering

Shi-Chao Lin(林世超), Xin Zhang(张鑫), Wei-Chen Zhao(赵伟臣), Zhao-Yang Chen(陈朝阳), Pan Du(杜攀), Yong-Mei Zhao(赵永梅), Zheng-Long Wu(吴正龙), Hai-Jun Xu(许海军)
Citation: Chin. Phys. B . 2018, 27(2): 028707. **doi:** 10.1088/1674-1056/27/2/028707

Journal homepage: http://cpb.iphy.ac.cn; http://iopscience.iop.org/cpb

What follows is a list of articles you may be interested in

A general method for large-scale fabrication of Cu nanoislands/dragonfly wing SERS flexible substrates

Yuhong Wang(王玉红), Mingli Wang(王明利), Lin Shen(沈琳), Yanying Zhu(朱艳英), Xin Sun(孙鑫), Guochao Shi(史国超), Xiaona Xu(许晓娜), Ruifeng Li(李瑞峰), Wanli Ma(马万里)
Chin. Phys. B . 2018, 27(1): 017801. **doi:** 10.1088/1674-1056/27/1/017801

Three-dimensional noble-metal nanostructure：A new kind of substrate for sensitive, uniform, and reproducible surface-enhanced Raman scattering

Tian Cui-Feng, You Hong-Jun, Fang Ji-Xiang
Chin. Phys. B . 2014, 23(8): 087801. **doi:** 10.1088/1674-1056/23/8/087801

An effective surface-enhanced Raman scattering template based on gold nanoparticle/silicon nanowire arrays

Wang Ming-Li, Zhang Chang-Xing, Wu Zheng-Long, Jing Xi-Li, Xu Hai-Jun
Chin. Phys. B . 2014, 23(6): 067802. **doi:** 10.1088/1674-1056/23/6/067802

Enormous enhancement of electric field in active gold nanoshells

Jiang Shu-Min, Wu Da-Jian, Wu Xue-Wei, Liu Xiao-Jun
Chin. Phys. B . 2014, 23(4): 047807. **doi:** 10.1088/1674-1056/23/4/0478070

Quantitative and sensitive detection of prohibited fish drugs by surface-enhanced Raman scattering*

Shi-Chao Lin(林世超)[1,2], Xin Zhang(张鑫)[1,2,†], Wei-Chen Zhao(赵伟臣)[1,2], Zhao-Yang Chen(陈朝阳)[2], Pan Du(杜攀)[1,2], Yong-Mei Zhao(赵永梅)[3], Zheng-Long Wu(吴正龙)[4], and Hai-Jun Xu(许海军)[1,2,‡]

[1] *Beijing Bioprocess Key Laboratory, Beijing University of Chemical Technology, Beijing* 100029, *China*
[2] *College of Science, Beijing University of Chemical Technology, Beijing* 100029, *China*
[3] *Engineering Research Center for Semiconductor Integrated Technology, Institute of Semiconductors, Chinese Academy of Sciences, Beijing* 100083, *China*
[4] *Analytical and Testing Center, Beijing Normal University, Beijing* 100875, *China*

(Received 14 September 2017; revised manuscript received 20 November 2017; published online 5 January 2018)

Rapid and simple detections of two kinds of prohibited fish drugs, crystal violet (CV) and malachite green (MG), were accomplished by surface-enhanced Raman scattering (SERS). Based on the optimized Au/cicada wing, the detectable concentration of CV/MG can reach 10^{-7} M, and the linear logarithmic quantitative relationship curves between log$I$ and log$C$ allows for the determination of the unknown concentration of CV/MG solution. The detection of these two analytes in real environment was also achieved, demonstrating the application potential of SERS in the fast screening of the prohibited fish drugs, which is of great benefit for food safety and environmental monitoring.

Keywords: surface-enhanced Raman scattering, crystal violet, malachite green, quantitative detection

PACS: 87.64.kp, 78.30.–j **DOI:** 10.1088/1674-1056/27/2/028707

1. Introduction

Some drugs, including crystal violet (CV) and malachite green (MG), can be used to keep the health of fish, but they all have bad effects on people.[1,2] CV, a kind of triphenylmethane dye, has been found to be quite effective as fungicide and biocide in the fishery industry owing to its splendid bactericidal effect. Though it can be used as anti-fungal additive in the production of feed to improve the health of living body, CV gives side-effects by biotransformation after entering into the human or animal body and is carcinogenic, teratogenic, mutagenic, and so on.[1] MG is a cationic triphenylmethane dye and can act as a drug to sterilize and kill parasites in aquaculture. Nevertheless, this substance is resistant to biodegradation and has serious carcinogenicity and genotoxicity.[2] Though being forbidden to be used in aquatic products,the abuse of both CV and MG cannot be stopped due to their low cost and high efficiency. In consequence, it is necessary to find an expeditious approach to realize the sensitive detection of trace amounts of CV and MG.

There are many methods to detect CV and MG, such as liquid chromatography–tandem mass spectrometer, gas chromatography–mass spectrometry, and high-performance liquid chromatography,[3,4] but they are either time-consuming or complicated. Compared with these methods, surface-enhanced Raman scattering (SERS) can realize rapid, simple, and inexpensive detection. In the past decades, SERS has gained much attention all around the world due to its characteristics of non-destructive testing feature, rapid response, sensitive detection and trace analysis ability. As a convenient tool, SERS is widely used in many fields of science, including food safety, environmental evaluation, biosensing and analytical chemistry.[5–7] Benefiting from the distinct enhancement of signal intensity, SERS can be used to analyze a substance at the single molecule level.[8] The enhancement effect is generally owing to a combination of the electromagnetic (EM) mechanism and the chemical mechanism, and the EM mechanism is predominant. To highly enhance the signal of the analyte molecules, noble metals, such as Au, Ag, and Pt, are needed to prepare SERS substrates, and simultaneously microstructure having dense nanogaps is desired to facilitate the formation of enormous hot spots[9] on the substrates. Qi Jiwei *et al.* fabricated high-performance SERS substrate with deep controllable sub-10-nm gap structure by depositing Au film on the cicada wing, but the reproducibility is hard to control because of the method of ion beam sputtering.[9] Ichiro Tanahashi and Yoshiyuki Harada fabricated naturally inspired SERS substrate by photocatalytically depositing silver nanoparticles on cicada wings, but the substrate is not stable enough to store because Ag is easily oxidized in air.[10] Though great enhancement has been achieved by fabricating complicated substrates, it is difficult to reach the goal of the quantitative detection of some specific analytes.

*Project supported by the National Basic Research Program of China (Grant No. 2014CB745100), the National Natural Science Foundation of China (Grant Nos. 21390202 and 21676015), and the Beijing Higher Education Young Elite Teacher Project.

†Corresponding author. E-mail: zhxin@mail.buct.edu.cn
‡Corresponding author. E-mail: hjxu@mail.buct.edu.cn

© 2018 Chinese Physical Society and IOP Publishing Ltd

In this study, using Au/cicada wing as SERS substrate, the quantitative detection of CV and MG was achieved. The detectable concentration of CV and MG can both attain as low as 10^{-7} M, and the logarithmic quantitative relationship is linear which can serve as a standard for the determination of the unknown concentration of CV/ MG solution. Furthermore, CV and MG can also be quantitatively determined in a real environment, indicating the practicability of the SERS technique for the CV/MG detection.

2. Experimental section

Cryptotympana atrata fabricius were purchased from Jia-Ying Art Museum of Entomology. Rhodamine 6G (R6G), crystal violet (CV), and malachite green (MG) were procured from J & K Scientific Ltd. Deionized water (18 MΩ) acquired from Beijing Chemical Works was used for all experiments. The water for aquatic product was taken from a local aquaculture market located near Huixinxijie Nankou Station of Beijing Subway, named Tianlihong market**.** All chemicals, unless otherwise noted, were of analytical grade and were used as received.

The typical morphologies of cicada wing and Au/cicada wing were observed by field emission scanning electron microscopy (FE-SEM) (JEOL JSM-7800F).

The aqueous solutions of 10^{-2}-M R6G, CV and MG were prepared first, and then they were diluted to lower concentrations. The SERS signals of R6G, CV, and MG were obtained after the 10-μL droplets evaporated naturally on the cut pieces of Au/cicada wing with dimensions of ~ 2 mm$\times \sim 2$ mm. All of the signals were acquired at room temperature in a LabRAM ARAMIS Raman system. The diameter of the light spot was ~ 1 μm and the incident power was 5 mW for R6G and 1.7 mW for CV and MG, respectively. All the data were averaged over 5 randomly selected positions.

3. Results and discussion

The cicada wing has homogeneous micropapillae structure on its surface, as shown in Fig. 1(a). According to the statistics of 50 different positions, the top diameter, top distance, bottom diameter, bottom distance, and the height of micropapillae are 70, 105, 145, 45, and 300 nm, respectively. Possessing three-dimensional (3D) orderly microstructure, the cicada wing has many outstanding properties, such as large specific surface area, high hydrophobicity and antireflection.[11] After depositing Au NPs onto cicada wings by electron beam evaporation, there is no obvious change of the regular microstructure which can be seen clearly in Fig. 1(b). It is worth noting that the deposition of Au NPs is uniform and unordered, therefore the substrate can generate amounts of nanogaps which are conducive to form enough hot spots to enhance the SERS signal.

The SERS spectra of R6G at different concentrations were checked to evaluate the SERS property of the Au/cicada wing, as shown in Fig. 1(c). The excitation wavelength for the detection of R6G was 532 nm because this wavelength is close to the electronic resonance wavelength of analyte.[12] The spectra were recorded with an accumulation time of 16 s and the spectral resolution was 1 cm^{-1}. The grating constant for the detection was 1200. It is distinctly found that the characteristic peaks of R6G are quite clear even though the concentration of R6G is down to 10^{-7} M. The peak of 1361-cm^{-1} is assigned to the aromatic C–C stretching vibrations.[13] The inset in Fig. 1(c) shows the logarithmic quantitative relationship curve between the integrated peak intensity centered at 1361 cm^{-1} and the concentration of R6G, and a linear relationship is fitted with $R^2 = 0.97241$. On the strength of this curve, the linear relationship between $\log I$ and $\log C$ can be seen expressly.

In order to calculate the enhancement factor (EF) of the substrate, series of R6G solution dropped on the Au/cicada wing were checked to ascertain the saturation value, upon which the concentration of R6G used for calculating EF could be determined, as exhibited in Fig. 1(d). The accumulation time and spectral resolution was the same as before and the grating constant was 600. To facilitate the estimation, the intensity of 1361-cm^{-1} peak with respect to different R6G concentrations was counted. In the light of Fig. 1(d), the signal reached saturation when the R6G concentration is 10^{-3} M, therefore R6G solution of 10^{-3} M was used to calculate the EF value. The formula used was as follows:[14,15] $\mathrm{EF} = (I_{\mathrm{SERS}}/I_{\mathrm{Raman}}) \times (N_{\mathrm{Raman}}/N_{\mathrm{SERS}})$, where I_{SERS} is the peak intensity in SERS spectra, I_{Raman} is the peak intensity in non-SERS Raman spectra, N_{Raman} and N_{SERS} are the numbers of R6G molecules on bare and Au-decorated cicada wings, respectively. N_{Raman} can be determined based on the concentration of R6G (10^{-3} M) and the illuminated volume (V_{illu}) of the Raman system. When operating the Raman detection, the laser spot size was ~ 1 μm and the penetration depth of the laser beam was ~ 3 mm, hence the value of V_{illu} was estimated to be 2.36×10^3 μm^3. As a consequence, the value of N_{Raman} was 1.42×10^9. To figure out N_{SERS}, an assumption was established that R6G molecules formed a monolayer on the surface of the substrate. Considering that the superficial area of an R6G molecule was ~ 2.0 nm^2 (1.37 nm$\times$1.43 nm) and the saturation concentration of R6G absorbed on the substrate was 10^{-3} M, N_{SERS} was predicted to be 3.93×10^5. According to the spectra of SERS and Raman, I_{SERS} and I_{Raman} were 5.99×10^4 and 5.37×10^3, respectively. Thus, the values of $I_{\mathrm{SERS}}/I_{\mathrm{Raman}}$ and $N_{\mathrm{Raman}}/N_{\mathrm{SERS}}$ were ~ 11.2 and $\sim 3.61 \times 10^3$, respectively, and the EF of the Au/cicada wing was calculated to be 4.03×10^4. This high EF value shows that the substrate is of great SERS enhancement performance.

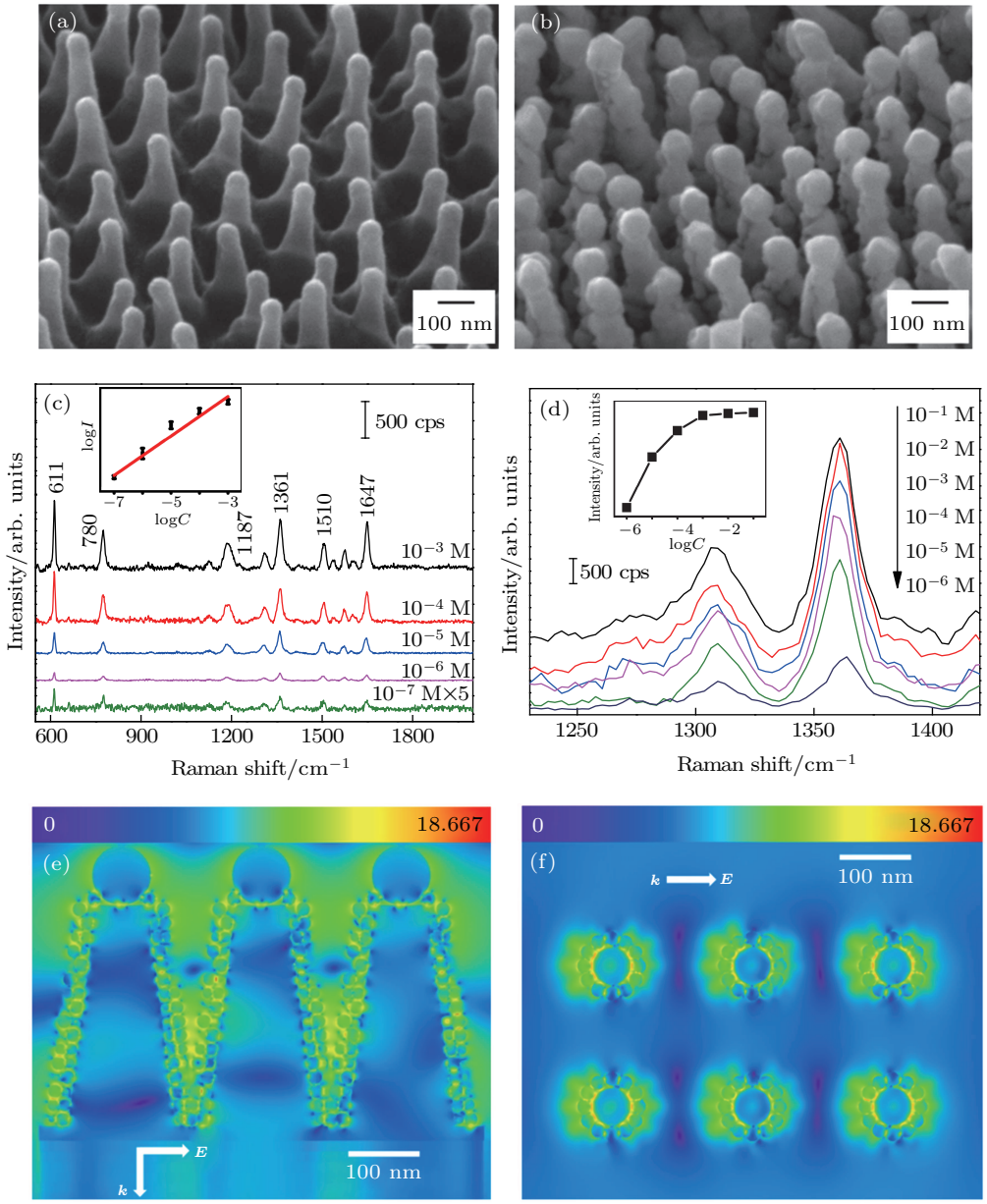


Fig. 1. (color online) FE-SEM micrographs of (a) bare cicada wing, and (b) Au/cicada wing, respectively. (c) SERS spectra of R6G solution at different concentrations. The inset is logarithmic quantitative relationship curve of the 1361-cm^{-1} peak intensities of R6G. (d) SERS spectra of R6G solution from 10^{-6} M to 10^{-1} M, with the inset showing the variation trend of the 1361-cm^{-1} peak intensities. (e) Simulated result of the distribution of the electric field intensity on *x*–*z* plane. (f) Simulated result of the distribution of the electric field intensity on *x*–*y* plane.

To testify the SERS performance of the Au/cicada wing theoretically, the finite-difference time-domain (FDTD) simulations of electric field distribution were conducted. Figure 1(e) shows the electric field distribution in *x*–*z* plane, where two kinds of hot spots can be found, including one between adjacent Au NPs and the other between neighboring protrusions. Figure 1(f) shows the electric field distribution in *x*–*y* plane, which passes across small Au NPs on the top of protrusions. The maximum simulated value of local electric field was 18.667 V/m, and the simulative EF was estimated to be 1.21×10^5, which is in basic accordance with the experimental data.

Using the Au/cicada wing substrate, SERS spectra of CV solutions with different concentrations were measured, and the result was shown in Fig. 2(a). The incident laser for CV was at 633 nm.[16] The spectra were recorded with an accumulation time of 16 s and the spectral resolution was 1 cm^{-1}. The grating constant for the detection was 600. The main Raman peaks at 916, 1174, 1381, and 1618 cm^{-1} are shown clearly. The peak located at 916 cm^{-1} is attributed to the skeleton vibration of radial aromatic ring. The 1174-cm^{-1} peak is assigned to the bending vibration of radial aromatic ring in the plane of C–H bond. The peak at 1381 cm^{-1} originates from the synergy of in-plane C–C stretching vibration and N-phenyl stretching. The peak at 1618 cm^{-1} corresponds to the in-plane C–C stretching vibration of the ring.[1,17] According to the spectra, when the concentration of CV is down to 10^{-7} M, the characteristic peaks of it can also be seen clearly, indicating

that the detection of CV reaches the concentration of 100 nM.

To achieve the quantitative detection of CV, the logarithmic relationship curve of the 1618-cm^{-1} peak intensity was plotted to serve as a standard. The linear relationship between log$I$ and log$C$ is obvious, which is important for determining the CV concentration in solution. In order to examine whether the method can be applied in real environment, two types of water, including for life (E1) and for aquatic product (E2), were employed. The water for life was obtained from tap water in our lab and that for aquatic product was from a local aquaculture market. These two samples showed no CV signal before adding it. After being spiked with CV of different concentrations (5×10^{-5} M for E1 and 5×10^{-6} M for E2), the characteristic peaks appeared in the spectra, and the values of the 1618-cm^{-1} peak intensity conformed to the quantitative relationship curve, as shown in Fig. 2(b), indicating that this method could be applied in a real environment.

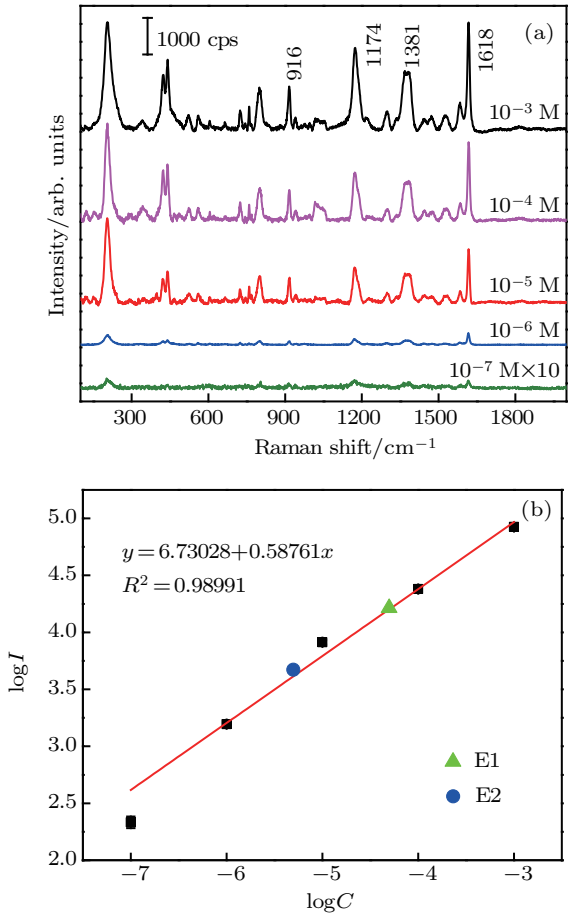


Fig. 2. (color online) (a) SERS spectra of CV solution at different concentrations. (b) Logarithmic quantitative relationship curve of the 1618-cm^{-1} Raman peak intensities of CV; the two added points stand for the results corresponding to two real environments: E1 (environment 1: water for life), and E2 (environment 2: water for aquatic product).

Figure 3(a) shows the SERS spectra of the MG solution with different concentrations from 10^{-7} M to 10^{-3} M. The test conditions for MG[2] were the same as for CV. It can be seen that the characteristic peaks of MG are still unambiguous even though its concentration reaches as low as 10^{-7} M, and the peaks are more obvious than the reported results obtained on an Ag decorated microstructured PDMS substrate.[18] The Raman peaks of 1176, 1367, and 1617 cm^{-1} are attributed to the ring C–H in-plane bending, N-phenyl stretching, and ring C–C stretching,[2] respectively. Figure 3(b) shows the logarithmic quantitative relationship curve of the 1617-cm^{-1} peak intensity of MG. The linear relationship between log$I$ and log$C$ allows for the determination of the concentration of an unknown MG solution. Moreover, the two real water samples which were ever used for CV detection, including water for life (E1) and water for aquatic product (E2), were spiked with MG of different concentrations (5×10^{-5} M for E1 and 5×10^{-6} M for E2) and then tested. The results accorded with the relationship curve, which is meaningful for the detection of MG in a real environment.

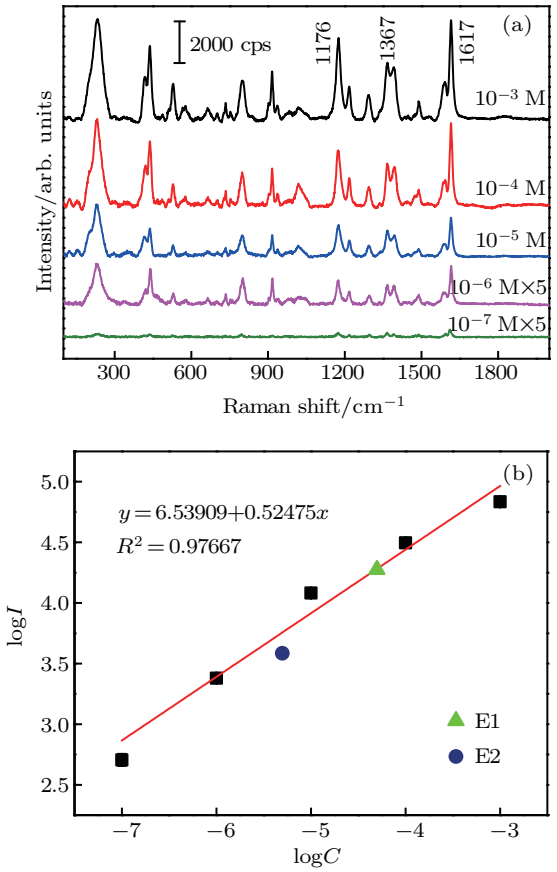


Fig. 3. (color online) (a) SERS spectra of MG solution at different concentrations. (b) Logarithmic quantitative relationship curve of the 1617-cm^{-1} Raman peak intensities of MG; the two added points stand for the results corresponding to two real environments: E1 (environment 1: water for life), and E2 (environment 2: water for aquatic product).

4. Conclusion and perspectives

In this study, the quantitative detection of two prohibited fish drugs was achieved using the sensitive SERS technology. The detectable concentration of both CV and MG can reach as low as 100 nM, and their logarithmic quantitative relationship curves show good linearity, allowing for the quantitative determination of unknown CV/MG concentrations in various

samples. The detection of CV/MG in a real environment was also demonstrated by SERS, which is of great importance for food safety and environmental protection.

References

[1] Senapati S, Srivastava S K, Singh S B and Kulkarni A R 2014 *Environ. Res.* **135** 95

[2] Song D, Yang R, Wang C W, Xiao R and Long F 2016 *Sci. Rep.* **6** 22870

[3] Halme K, Lindfors E and Peltonen K 2004 *Food Addit. Contam.* **21** 641

[4] Bueno M J M, Herrera S, Uclés A, Agüera A, Hernando M D, Shimelis O, Rudolfsson M and Fernández-Alba A R 2010 *Anal. Chim. Acta* **665** 47

[5] Zhang C X, Liu L, Yin H J, Fang H, Zhao Y M, Bi C J and Xu H J 2014 *Appl. Phys. Lett.* **105** 011905

[6] Fang H, Zhang C X, Liu L, Zhao Y M and Xu H J 2015 *Biosens. Bioelectron.* **64** 434

[7] Hou M J, Zhang X, Cui X Y, Liu C, Li Z C and Zhang Z J 2015 *Chin. Phys. B* **24** 034203

[8] Xu B B, Zhang Y L, Zhang W Y, Liu X Q, Wang J N, Zhang X L, Zhang D D, Jiang H B, Zhang R and Sun H B 2013 *Adv. Opt. Mater.* **1** 56

[9] Qi J W, Li Y D, Yang M, Wu Q, Chen Z Q, Wang W D, Lu W Q, Yu X Y, Xu J J and Sun Q 2013 *Nanoscale Res. Lett.* **8** 437

[10] Tanahashi I and Harada Y 2014 *Nanoscale Res. Lett.* **9** 298

[11] Morikawa J, Ryu M, Seniutinas G, Balčytis A, Maximova K, Wang X W, Zamengo M, Ivanova E P and Juodkazis S 2016 *Langmuir* **32** 4698

[12] Lamberti A, Virga A, Angelini A, Ricci A, Descrovi E, Cocuzza M and Giorgis F 2015 *Rsc Adv.* **5** 4404

[13] Tsai Y C, Hsu P C, Lin Y W and Wu T M 2009 *Sensor. Actuat. B-Chem.* **138** 5

[14] Li W Y, Camargo P H C, Lu X M and Xia Y N 2009 *Nano Lett.* **9** 485

[15] Chen L Y, Yang K H, Chen H C, Liu Y C, Chen C H and Chen Q Y 2014 *Analyst* **139** 1929.

[16] Song J, Huang Y Q, Fan Y X, Zhao Z H, Yu W S, Rasco B A and Lai K Q 2016 *Nanomaterials* **6** 175

[17] Li B, Shi Y E, Cui J C, Liu Z, Zhang X L and Zhan J H 2016 *Anal. Chim. Acta* **923** 66

[18] Kumar P, Khosla R, Soni M, Deva D and Sharma S K 2017 *Sensor. Actuat. B-Chem.* **246** 477